

## Accepted Manuscript

A novel and effective anchorage system for enhancing the flexural capacity of rc beams strengthened with frcm composites

Zena R. Aljazaeri, Michael A. Janke, John J. Myers

PII: S0263-8223(18)33417-2  
DOI: <https://doi.org/10.1016/j.compstruct.2018.10.110>  
Reference: COST 10362

To appear in: *Composite Structures*

Received Date: 20 September 2018

Revised Date: 23 October 2018

Accepted Date: 31 October 2018



Please cite this article as: Aljazaeri, Z.R., Janke, M.A., Myers, J.J., A novel and effective anchorage system for enhancing the flexural capacity of rc beams strengthened with frcm composites, *Composite Structures* (2018), doi: <https://doi.org/10.1016/j.compstruct.2018.10.110>

This is a PDF file of an unedited manuscript that has been accepted for publication. As a service to our customers we are providing this early version of the manuscript. The manuscript will undergo copyediting, typesetting, and review of the resulting proof before it is published in its final form. Please note that during the production process errors may be discovered which could affect the content, and all legal disclaimers that apply to the journal pertain.



25 FRCM composite. Real-scale simply supported RC beams were examined under the  
26 effect of strengthening with different reinforcement ratios and with and without  
27 anchorage systems engagement. Test results revealed the contribution of anchorage  
28 systems in preventing or delaying the FRCM debonding failure mechanism and  
29 enhancing the flexural performance of strengthened beams.

30 Keywords: Anchorage; U-wrapped PBO anchorage; glass spike; FRCM strengthening;  
31 flexural behavior.

## 32 1. Introduction and Background

33 Different types of anchorage systems have been used to delay the premature  
34 debonding failure mode associated with FRP composites. The successful anchorage  
35 systems have allowed the FRP's composite materials to continuously carry a load in  
36 shear or flexure in which extra benefits from high-strength fabrics were achieved. Thus,  
37 proper anchorage systems can reduce the required cross-sectional area of the  
38 expensive fabric materials or provide a better structural performance with respect to  
39 increasing in the fabrics reinforcement ratio. Some of the important anchor types are  
40 mechanical anchorages, U-wrapped sheets, anchor spikes, and FRP rods. Many  
41 experimental studies have illustrated the efficiency and applicability of these anchorage  
42 systems. Khalifa et al. [1] invented a novel anchor that was used to reduce the stress  
43 concentration of FRP systems at the ends. The novel anchor consisted of FRP sheets  
44 that were extended through a groove filled with epoxy that may or may not include an  
45 FRP rebar. Khalifa et al. [1] stated that "the u-anchor system provides an effective  
46 solution for cases in which the bonded length of FRP composites is not sufficient to  
47 develop its full capacity." Wu and Huang [2] and You et al. [3] used mechanical

48 anchorages with FRP composites. The authors concluded that the mechanical anchors  
49 for prestressed FRP strips allowed higher flexural loads and ductile behavior  
50 enhancement. It was also concluded that the anchored beams experienced a rupture in  
51 the FRP strips as the anchors were successfully preventing the FRP strips from  
52 debonding. Kim et al. [4] replaced the mechanical anchors for prestressed FRP sheets  
53 with nonmetallic anchorages (non-anchored U-wrap and anchored U-wrap). The test  
54 results concluded the efficiency of the replaced nonmetallic anchors at maintaining a  
55 considerable amount of prestressing force in FRP sheets. Bae and Belarbi [5]  
56 determined the improving effect of three mechanical anchorage types in shear-  
57 strengthened RC beams. Piyong et al. [6] and Smith et al. [7] used glass fiber spikes to  
58 enhance the flexural performance of concrete slabs strengthened with nonprestressed  
59 and prestressed carbon-FRP sheets. The test results indicated that the glass anchor  
60 spikes significantly increased the ultimate strength and the ductility of the strengthened  
61 slabs. The rupture of fibers was captured at the ultimate stage instead of the fibers  
62 debonding. Smith et al. [7], Ekenel et al. [8], and Ekenel and Myers [9] conducted  
63 studies on the glass spikes to anchor FRP sheets for flexural strengthening RC beams.  
64 Two of the studies determined the effectiveness of using glass anchor spikes on  
65 upgrading the flexural strength of RC beams. However, the anchor spikes did not  
66 contribute to the flexural stiffness of strengthened RC beams subjected to fatigue  
67 loading [9]. Despite all of the above research, this new generation of FRCM composite  
68 materials are still under investigation to be implemented for repair and strengthening of  
69 infrastructure systems. The FRCM composite material consists of a fabric made of  
70 either carbon, polyparaphenylene benzobisoxazole (PBO), or glass and a cement

71 based mortar. This type of composite has distinct properties that overcome the FRP  
72 composites such as resistance to elevated temperature, non-toxic fume installation,  
73 compatibility with structural materials (concrete and masonry), and high impact  
74 resistance [10, 11, 12]. The FRCM composites have been investigated through many  
75 researches to determine its effectiveness in flexure, shear, and fatigue performance [10,  
76 11, 12, 13, 14, 15, 16]. Experimental studies determined that increasing the  
77 reinforcement ratio of FRCM composite was not proportionally increased the load  
78 carrying capacities of RC members. The debonding failure mode was announced for all  
79 repaired or strengthened RC members with multilayers of FRCM [10, 11, 12, 13, 14, 15,  
80 16]. Thus, experimental studies are necessary to examine the effectiveness of using  
81 anchorage systems with FRCM system. However, limited experimental researches are  
82 presented here. A novel textile-based anchor was developed by Tetta et al. [17] and  
83 used to improve the textile reinforced mortar (TRM) composite in the shear  
84 strengthening of T-section RC beams. The novel anchor consisted of fan-shaped textile  
85 strips that doveled into concrete at one end and distributed over the U-wrapped  
86 strengthening system. The fan strips served for the distribution of stresses between the  
87 textile reinforcements and the anchored strips. The dowel part of the anchor served for  
88 fixing the fan-shaped anchors into the concrete mass. The effect of the anchorage  
89 number, position of anchors, textile type, and textile layers was studied. The test results  
90 defined the great influence of textile anchorage in shear strength gain. Younis et al. [18]  
91 studied different FRCM systems for shear strengthening application. Some beams were  
92 strengthened with FRCM system and anchored at the top and bottom with FRP plate in  
93 order to increase the efficiency of FRCM in shear enhancement. In spite of using

94 anchorage, the measured load carrying capacity of the anchored FRCM was  
95 insignificant. Marcinczak and Trapko [19] evaluated the influence of using U-wrapped  
96 stirrups of FRCM in shear strengthening of beams. The U-stirrups anchorage was able  
97 to increase the shear capacity of the strengthened beams in the range of 15% to 27% of  
98 that of unstrengthen beam. However, the proposed method of anchoring did not ensure  
99 a complete utilization of tensile strength of the PBO mesh. More work are in need to  
100 understand the effect of using anchorage systems and which types would be an  
101 effective technique. This work represents a pilot study to investigate the effect of using  
102 different anchorage systems to improve the flexural performance of strengthened  
103 beams with an FRCM system.

## 104 **2. Research Significance**

105 This work is a pilot study on using anchorage systems with cement-based composites.  
106 The idea behind using anchorage systems is based on the observed debonding failure  
107 mode in many experimental works for strengthened RC beams with multilayers of  
108 FRCM composite. The aims of this study were to determine the influence of anchorage  
109 systems on increasing the flexural performance of FRCM composite either by delay or  
110 prevent the debonding in FRCM composite and to determine whether the anchorage  
111 systems would influence the failure type of the FRCM composite or not.

## 112 **3. Experimental Work**

### 113 **3.1 Material properties**

114 The experimental program included a total of seven medium-scale beams. The RC  
115 beams had nominal cross-sectional dimensions of 305 mm (12-in.) depth and 203 mm  
116 (8-in.) width with a total length of 2.133 m (7-ft). The concrete was ready-mixed

117 concrete with 28-day target strength of 41.4 MPa (6,000 psi). Concrete cylinders that  
118 had a diameter of 100 mm (4-in.) and a height of 200 mm (8-in.) were used to specify  
119 the concrete properties. The compressive strength and young's modulus of elasticity of  
120 concrete were based on ASTM C39 [20] and ASTM C469 [21], respectively. The  
121 concrete's average compressive strength of three tested cylinders was about 45.5 MPa  
122 (6,600 psi) at the date of the beam specimens' testing, and the concrete's modulus of  
123 elasticity was about 36,425 MPa (5,283 ksi). Steel rebar of 10 mm (No. 3) in diameter  
124 was used as longitudinal and transverse reinforcements. The tensile yield and ultimate  
125 strengths were determined by testing three coupon specimens based on ASTM A370  
126 [22]. The average yield strength of three coupons was 482 MPa (70 ksi), and the  
127 average ultimate rupture of three coupons was 726 MPa (105 ksi). The  
128 polyparaphenylene benzobisoxazole (PBO) fabric was the proposed type of FRCM  
129 composite in this study. The PBO fabric was made of 5 mm (0.2-in.) and 3 mm (0.125-  
130 in.) wide yarns in the longitudinal and transverse directions, respectively, as shown in  
131 Fig.1.1. The free space between the yarns was roughly 5 mm (0.2-in.) and 22 mm (0.9-  
132 in.) in the longitudinal and transverse directions, respectively, and the nominal thickness  
133 of the yarns was 0.2 mm (0.008-in.) and 0.12 mm (0.045-in.) in the longitudinal and  
134 transverse directions, respectively. The cement-based mortar was made of a  
135 combination of Portland cement, silica fume, and fly ash as a binder. It had less than 5  
136 percent polymer. The cement-based mortar also contained glass fibers to improve the  
137 bond between the PBO mesh and the cement mortar and to provide better tensile  
138 properties. The other type of cement mortar was used as a base mortar to level the  
139 concrete surface, close the crack opening, and improve the bond performance between

140 the FRCM composite and the concrete substrate. The base mortar was made of fine  
141 cement particles and silica fume. The base mortar contained polypropylene fibers to  
142 bridge concrete cracks and to improve the bond performance of the FRCM composite-  
143 concrete surfaces. All FRCM composite materials are presented in Fig. 1. The PBO  
144 fabric was used as external flexure reinforcement with a tensile strength of 5,800 MPa  
145 (840 ksi), elastic modulus of 270,000 MPa (39,160 ksi), and ultimate strain of 0.0215  
146 mm/mm (in./in.). All of the beams were designed to fail in flexure based on the ACI 549-  
147 13 [23] and ACI 318-14 [24]. A typical beam dimensions and its internal reinforcement  
148 details are presented in Fig. 2.

### 149 **3.2 Strengthening schemes**

150 Two different anchorage systems were considered in this study. The first anchorage  
151 system was the glass spike. As mentioned above, the glass spike was used in previous  
152 research and successfully enhanced the FRP composite's flexural performance [6, 9].  
153 The second anchorage system was a novel U-wrapped PBO strip. A new technique of  
154 anchoring the U-wrapped PBO strips is proposed to inhibit the debonding of the U-  
155 wrapped PBO strip by transferring the stresses into concrete, as presented in section  
156 3.3. Two strengthening reinforcement ratio were considered here. Three RC beams  
157 were strengthened with two FRCM sheets and the other three beams were  
158 strengthened with three FRCM sheets. Two sheets of FRCM strengthening with  
159 anchorage systems were selected in order to determine its ability to replace four FRCM  
160 sheets. Four sheets of FRCM strengthening with anchoring systems were designed in  
161 order to delay the premature debonding failure of four FRCM sheets and examine  
162 higher order enhancements in flexural performance. Table 1 summarizes the test matrix



163 of seven RC beams. One RC beam specimen served as the control beam. The other  
164 beam specimens were divided into two groups of three beam specimens. In group one,  
165 beams were strengthened with two sheets of FRCM composite. In group two, beams  
166 were strengthened with four sheets of FRCM composite. In each group, one beam was  
167 strengthened with FRCM composite without anchorages, one beam was strengthened  
168 with FRCM composite and anchored with glass spikes, and one beam was  
169 strengthened with FRCM composite and anchored with U-wrapped PBO strips. Seven  
170 anchors were spaced along the span length of the strengthened beams. The number of  
171 anchors was distributed through the beam span length to reduce the stress concentration  
172 at the maximum moment regions and at the ends of FRCM strengthening where not  
173 enough development length was provided. The center-to-center spacing between the  
174 anchors was 280 mm (11-in.). The distribution and detail of glass spikes are presented  
175 in Fig. 3a. The central position of glass spikes were extended 25.4 mm (1.0-in.) from the  
176 center line of RC beams in a staggered form in order to prevent drilling at the location of  
177 longitudinal rebar. The glass spike width was 150 mm (6-in.). The U-wrapped PBO  
178 strips' width was 114 mm (4.5-in.). The U-wrapped PBO strips were anchored into the  
179 sides of RC beams at a depth of 100 mm (4.0-in.) from the top concrete surface to be  
180 away from the maximum tensile and compressive stresses areas, as shown in Fig. 3b.  
181 The anchor material mechanical properties are presented in Table 2. The detailed  
182 schemes for anchorage systems are presented in Fig. 4. The anchor's diameter was 15  
183 mm (0.6-in.) and the embedded length inside the concrete was 50 mm (2-in.) for each  
184 anchorage system.

### 185 **3.3 Anchorage systems preparation and strengthening application**

186 Before the FRCM strengthening system was applied on the RC beams' substrates, all  
187 beams were pre-cracked to 65% of their expected ultimate load capacity. This level of  
188 load represented an approximate service loading level based on the ACI 549-13 [23].  
189 Then, the beams were sandblasted to remove the smooth layer of concrete surface and  
190 provide better surface to adhere the FRCM composite as recommended by the ACI  
191 549-13 [23]. The edges of two RC beams were rounded to 20 mm (0.75-in.) in order to  
192 reduce the stress concentrations around the U-wrapped PBO strips as recommended  
193 by the ACI 549-13 [23]. Holes that were 50 mm (2-in.) long and 18 mm (0.7-in.) in  
194 diameter were drilled into the concrete at the desired points for installing the anchorage  
195 systems. All of the holes were cleaned with air pressure and all of the beams' surfaces  
196 were vacuumed to remove the dust. The anchorage systems were prepared as follows.  
197 The first anchor type was the glass spike. The glass spike was made by cutting a strip  
198 of the glass filament from the roving roll and folding several times to provide the  
199 required diameter, as shown in Fig. 5a. The folded ends of the glass strip were cut to  
200 have a total length of 254 mm (10-in.). One end was saturated using an epoxy agent  
201 (Mbrace<sup>TM</sup>-saturant) to be doveled inside the concrete hole with a bond length of 50  
202 mm (2-in.), as shown in Fig. 5 (b and c). The glass spikes left to be set for more than  
203 four hours at a laboratory temperature based on manufacture requirement. Then the  
204 glass spikes were attached to the concrete holes by epoxy agent and left to be set for  
205 four hours, as shown in Fig. 5d. After that, the installation of the FRCM composite  
206 began by wetting the concrete substrate to eliminate the water absorption from the  
207 applied cement-based mortar. The FRCM strengthening in the form of two or four PBO  
208 sheets was applied to the concrete substrate. The cement-based mortar was used

209 successively to attach the PBO sheets, as shown in Fig. 6 (a, b, and c). The PBO  
210 sheets had a width of 200 mm (7.5- in.) and a length of 1830 mm (72-in.). The glass  
211 anchor spikes were fanned over the last layer of the PBO sheet in a circular pattern, as  
212 shown in Fig. 6d, and covered with the cement-based mortar, as shown in Fig. 6e.

213 The second anchor type was the novel U-wrapped PBO strip. The U-wrapped PBO strip  
214 was made by cutting the PBO fabric in strips and removing the PBO fabric in the  
215 transverse direction, as shown in Fig. 7 (a and b). Then, the ends of the PBO strips  
216 were saturated with epoxy agent (Mbrace-saturant) for a length of 50 mm (2-in.) to be  
217 anchored in RC beams, as shown in Fig. 7 (c, d, and e). The installation of the U-  
218 wrapped PBO strips was done immediately after applying the successive layers of the  
219 FRCM composite, as shown in Fig. 8 (a, b, and c). Then, the U-wrapped PBO strips'  
220 ends were adhered into concrete holes using a high viscosity gel epoxy (MasterEmaco,  
221 ADH 1420), as shown in Fig. 8d. The final shape of the U-wrapped PBO strip is  
222 presented in Fig. 8e. All of the strengthened RC beams were cured with water for three  
223 days and covered with plastic sheets to prevent the loss of moisture. Then, the  
224 strengthened RC beams were cured under laboratory conditions for 25 additional days  
225 before testing. The curing steps of the applied FRCM composite and anchorage  
226 systems were performed in the regards of manufactures recommendation.

#### 227 **4. Test Set-up and Instrumentation**

228 Four-point loading was selected to determine the anchorages' efficiency. The loads  
229 were applied on a displacement rate control of 1.3 mm/minute (0.05 in./min). A linear  
230 variable differential transducer (LVDT) was used to measure the displacement in the RC  
231 beams. Strain gauges were used to determine the strain reading of the internal

232 longitudinal rebar and the external applied FRCM composite. The distribution schemes  
233 of strain gauges are presented in Fig. 9.

234 For all RC beams, two strain gauges were bonded to the longitudinal rebar at the mid-  
235 span, two strain gauges were bonded to first and last sheets of the FRCM composite at  
236 the mid-span, and three strain gauges were attached to the external surface of the  
237 FRCM composite (at the mid-span and at the ends), as shown in Fig. 9a. For the U-  
238 wrapped PBO strips, five strain gauges were attached to each PBO strip to determine  
239 its effective strain at the bottom, the edge region, and area close to the anchored ends,  
240 as shown in Fig. 9b. The data acquisition system was used to record the load  
241 displacement curve and the strain gauge readings.

## 242 **5. Experimental Results**

### 243 **5.1 Load displacement**

244 The load displacement curves of tested beams are presented in Fig. 10. Table 3  
245 includes the key results: ultimate load, percentage increase in ultimate load,  
246 displacement at yielding of rebar, displacement at ultimate load, and displacement  
247 ductility index. The load displacement response for the control RC beam was a classic  
248 response. The rebar yielded at 72 kN (16 kips) followed by an ultimate load of 122 kN  
249 (27.4 kips). Then, the load displacement curve turned to the plastic-ductile response  
250 and the concrete crushing terminated the test. The strengthened beams exhibited a  
251 gain in the flexure strength through the inelastic loading stage followed by a drop in their  
252 carrying loads as the FRCM strengthening and anchorage systems reached their failure  
253 loads. Then, the strengthened beams went through the plastic-ductile stage similar to  
254 the control beam. The strengthened beams with two and four PBO sheets produced

255 higher ultimate loads of 154 kN (34.6 kips) and 141 kN (31.6 kips), respectively. The  
256 anchored beams with glass spikes carried an ultimate load of 147 kN (33 kips) and 154  
257 kN (34.6 Kips) for two and four PBO sheets, respectively. The anchored U-wrapped  
258 beams supported an ultimate load of 148 kN (33.3 kips) and 175 kN (39.2 kips) for two  
259 and four PBO sheets, respectively. It is concluded that the anchorage systems were  
260 more effective when a higher reinforcement ratio of PBO sheets was provided. As a  
261 measurement for the ductility performance of the strengthened beams with and without  
262 anchorages, the displacement ductility index was determined. The displacement  
263 ductility index represented the ratio of the beam's displacement at the ultimate load to  
264 the beam's displacement at the yielded load. The strengthened beams with and without  
265 anchorages obtained lower displacements at the yielded and ultimate load stages with  
266 respect to the control beam. However, most strengthened beams retained 65% to 87%  
267 displacement ductility index of that of the control beam with the exception of the  
268 strengthened beam with four PBO sheets which had only 45% displacement ductility  
269 index of that of the control beam due to the premature FRCM debonding. In addition,  
270 the effectiveness of the anchorage systems on the displacement ductility performance  
271 increased for the strengthened beams with four PBO sheets than two PBO sheets.  
272 Thus, the anchorage systems had a better ductile behavior as the FRCM reinforcement  
273 ratio increased.

## 274 **5.2 Crack pattern, failure mode, and number of sheets**

275 All of the beams failed due to flexural cracks that observed from the tensile face toward  
276 the top face of the beams, preceded by FRCM strengthening failure, as shown in Fig.  
277 11. In addition, concrete crushing was noticed at the final loading stage. The non-

278 anchored beams that were strengthened with two or four sheets of FRCM composite  
279 exhibited intermediate debonding at the maximum loaded area and the endplate  
280 debonding at the free end. The debonding was at the interface between the PBO sheets  
281 and the cementitious matrix. The anchored beam with glass spikes that was  
282 strengthened with two sheets of FRCM composite exhibited a slippage of the PBO  
283 sheets out of the cementitious matrix at the mid-span with no debonding of the PBO  
284 sheets along the span length. The anchored beam with glass spikes that was  
285 strengthened with four sheets of FRCM composite was revealed intermediate  
286 debonding and endplate debonding of the PBO sheets out of the cementitious matrix.  
287 The anchored beams with U-wrapped PBO strips that were strengthened with two  
288 sheets of FRCM composite exhibited a slippage of the PBO sheets and U-wrapped  
289 PBO strips out of the cementitious matrix at the mid-span. A slippage failure mode of  
290 the PBO sheet usually indicates that the PBO fabric developed a higher percentage of  
291 its tensile strength. In such a case, anchorage systems could not contribute more in  
292 upgrading the flexural performance of strengthened beams. However, the mode of  
293 failure was improved from intermediate debonding and end plate debonding to the  
294 slippage of PBO sheets, while anchorage systems contributed to delay the premature  
295 debonding failure mode and increase the ultimate loads in strengthened beams with  
296 four PBO sheets. The ultimate load of the strengthened beam with four PBO sheets and  
297 anchored with glass spikes was 10% higher than the non-anchored strengthened beam  
298 with four PBO sheets. The ultimate load of the strengthened beam with four PBO sheets  
299 and anchored with U-wrapped PBO strips was 24% higher than the non-anchored  
300 strengthened beam with four PBO sheets.

### 301 **5.3 Anchorage's configuration and material**

302 Test results of anchored beams determined different flexural performance. The external  
303 reinforcement ratio of the PBO sheets was interfered with the contribution of the  
304 anchorage systems. The glass spikes contributed to reduce the stress concentration in  
305 the direction of the PBO sheets and delayed the debonding failure mode. The anchored  
306 U-wrapped PBO strips performance verified the research idea of relying on the high-  
307 tensile strength of PBO strips. The ends of the PBO strips which anchored into the  
308 concrete prevented the debonding of the U-wrapped PBO strips, and developed a  
309 slippage failure mode in the PBO strips. The anchored U-wrapped PBO strips resulted  
310 in greater enhancement than glass spikes in terms of the ultimate load and the  
311 displacement ductility of the strengthened beam with four PBO sheets. The anchorage  
312 and confinement of the anchored U-wrapped PBO strips contributed to its greater  
313 impact. In addition, the anchors' material type could also play role in the efficiency of the  
314 anchorage systems. The PBO strips had higher tensile properties than glass spikes,  
315 which could be another reason why the U-wrapped PBO strips performed better. More  
316 experimental investigation would assist in a proper selection of the anchorage systems  
317 in terms of the material type and configuration.

### 318 **5.4 Strain measurements**

319 Measurements of the strains in the rebar, FRCC strengthening, and U-wrapped PBO  
320 strips are presented in Table 4. The strain reading of the rebar determined that it was  
321 yielded in all tested beams. The ultimate strain in the rebar ranged between 0.005  
322 mm/mm (in./in.) and 0.006 mm/mm (in./in.) based on the measurement of two beams.  
323 The strain reading in the first applied PBO sheet at mid-span ranged between 0.002

324 mm/mm (in./in.) and 0.005 mm/mm (in./in.), while higher strain readings were obtained  
325 in the last applied PBO sheet at mid-span. The anchorage systems reduced the strain  
326 reading of the PBO sheets at the edges. Glass spikes reduced the strain reading of the  
327 PBO sheets by half of that measured in strengthened beams without glass spikes. The  
328 U-wrapped PBO strips at the edges showed zero strain reading in the PBO sheets. The  
329 non-strain reading of the PBO sheets at the edges indicated the influence of the  
330 anchorage systems in preventing the PBO sheets' endplate debonding.

## 331 **6. Conclusions**

332 Anchorage systems can be used in order to delay or prevent debonding of the  
333 composite materials from concrete substrate in flexural strengthening or repairing  
334 applications. In such applications, the debonding can occur at the maximum moment  
335 regions or when not enough development length of strengthening systems can be  
336 provided. Prevent the debonding would maintain the structural efficiency. The  
337 effectiveness of two anchorage systems in increasing the strength and displacement  
338 ductility of FRCM strengthened RC beams is reported as follows:

- 339 1. The anchorage systems can enhance the flexural performance of strengthened RC  
340 beams with FRCM composite based on the provided strengthening reinforcement  
341 ratio.
- 342 2. The anchorage systems successfully prohibited the endplate debonding failure  
343 mode where not enough development length could be provided.
- 344 3. The anchorage systems were proved to prevent or delay the intermediate debonding  
345 failure mode in the FRCM strengthening based on its reinforcement ratio.



- 346 4. The non-anchored and anchored strengthened beams with two PBO sheets  
347 obtained the same flexural strength but the anchorage systems changed the mode  
348 of failure from a debonding failure to a slippage failure of the PBO sheets.
- 349 5. The novel anchored U-wrapped PBO strips increased the ultimate load by 24% more  
350 than the non-anchored strengthened beam with four PBO sheets.
- 351 6. The anchored U-wrapped PBO strip had a superior flexural enhancement compared  
352 to the glass spike due to its high tensile property and confinement action.

### 353 **Acknowledgments**

354 This work was supported by Ruredil Company and the ReCAST Tier 1 University  
355 Transportation Center at Missouri S&T. The authors acknowledge greatly both  
356 resources for their financial support. As well as to the academic support from the Center  
357 for Infrastructure Engineering Studies and the Department of Civil, Architectural, and  
358 Environmental Engineering at Missouri S&T. Any opinions, findings, conclusions, and  
359 recommendations presented in this paper are those of the authors and do not  
360 necessarily reflect the views of the sponsor or supporting agencies.

### 361 **References**

- 362 1. Khalifa, A., Alkhrdaji, T., Nanni, A., and Lansburg, S. (1999). "Anchorage of surface  
363 mounted FRP reinforcement." *Concrete International*, 21(10), 49-54.
- 364 2. Wu, Y. F., and Huang, Y. (2008). "Hybrid bonding of FRP to reinforced concrete  
365 structures." *Journal of Composites for Construction*, 12(3), 266-273.
- 366 3. You, Y. C., Choi, K. S., and Kim, J. (2012). "An experimental investigation on flexural  
367 behavior of RC beams strengthened with prestressed CFRP strips using a durable  
368 anchorage system." *Composites Part B: Engineering*, 43(8), 3026-3036.

- 369 4. Kim, Y. J., Wight, R. G., and Green, M. F. (2008). "Flexural strengthening of RC  
370 beams with prestressed CFRP sheets: Development of nonmetallic anchor  
371 systems." *Journal of Composites for Construction*, 12(1), 35-43.
- 372 5. Bae, S. W., and Belarbi, A. (2012). "Behavior of various anchorage systems used for  
373 shear strengthening of concrete structures with externally bonded FRP sheets."  
374 *Journal of Bridge Engineering*, 18(9), 837-847.
- 375 6. Piyong, Y., Silva, P. F., and Nanni, A. (2003). "Flexural strengthening of concrete  
376 slabs by a three-stage prestressing FRP system enhanced with the presence of  
377 GFRP anchor spikes." *Proceedings of the International Conference Composites in*  
378 *Construction (CCC 2003-Vol. 239244)*.
- 379 7. Smith, S. T., Hu, S., Kim, S. J., and Seracino, R. (2011). "FRP-strengthened RC  
380 slabs anchored with FRP anchors." *Engineering Structures*, 33(4), 1075-1087.
- 381 8. Ekenel, M., Rizzo, A., Myers, J., and Nanni, A. (2006). "Flexural fatigue behavior of  
382 reinforced concrete beams strengthened with FRP Fabric and precured laminate  
383 systems." *Journal of Composite for Construction*, 10, 443-442.
- 384 9. Ekenel M. and Myers J.J. (2009)." Fatigue performance of CFRP strengthened RC  
385 beams under environmental conditioning and sustained load." *Journal of*  
386 *Composites for Construction*, 13(2), 93-102.
- 387 10. Ombres, L. (2011). "Flexural analysis of reinforced concrete beams strengthened  
388 with cement based high strength composite material." *Composite Structures*, 94(1),  
389 143-155.
- 390 11. Loreto, G., Leardini, L., Arboleda, D. and Nanni, A. (2013). "Performance of RC slab-  
391 type elements strengthened with fabric-reinforced cementitious-matrix composites."

- 392 Journal of Composites for Construction, 10.1061/(ASCE) CC.1943-5614.0000415,  
393 18(3), A4013003-1.
- 394 12. Aljazaeri, Z., and Myers, J.J., (2016). "Fatigue and flexural behavior of reinforced  
395 concrete beams strengthened with a fiber reinforced cementitious matrix." ASCE  
396 Journal of Composites for Construction, 10.1061/(ASCE)CC.1943-5614.0000696.
- 397 13. Babaeidarabad, S. Loreto, G. and Nanni, A. (2014). "Flexural strengthening of RC  
398 beams with an externally bonded fabric-reinforced cementitious matrix." ASCE  
399 Journal of Composites for Construction, 10.1061/(ASCE)CC.1943-5614.0000473,  
400 18(5), 04014009-1.
- 401 14. Loreto, G., Babaeidarabad, S., Leardini, L., and Nanni, A., (2015). "RC beams  
402 shear-strengthened with fabric-reinforced cementitious-matrix (FRCM) composite."  
403 Int. J Adv. Struct. Eng. (IJASE), 7(4), 341-352.
- 404 15. Aljazaeri, Z., and Myers, J.J., (2017). "Strengthening of Reinforced-Concrete Beams  
405 in Shear with a Fabric-Reinforced Cementitious Matrix." Journal of Composites for  
406 Construction, 2017, 21(5): 04017041.
- 407 16. Aljazaeri, Z. R., & Myers, J. J. (2018). "Flexure Performance of RC One-Way Slabs  
408 Strengthened with Composite Materials." Journal of Materials in Civil  
409 Engineering, 30(7), 04018120.
- 410 17. Tetta, Z. C., Koutas, L. N., and Bournas, D. A. (2015). "Textile-reinforced mortar  
411 (TRM) versus fiber-reinforced polymers (FRP) in shear strengthening of concrete  
412 beams." Composites Part B: Engineering, 77, 338-348.

- 413 18. Younis, A., Ebead, U., and Shrestha, K. C. (2017). "Different FRCC systems for  
414 shear-strengthening of reinforced concrete beams." *Construction and Building*  
415 *Materials*, 153, 514-526.
- 416 19. Marcinczak, D., and Trapko, T. (2018). "Experimental research on RC beams  
417 strengthened in shear with PBO-FRCC composites." In *IOP Conference Series:*  
418 *Materials Science and Engineering* (Vol. 365, No. 4, p. 042035). IOP Publishing.
- 419 20. ASTM C39 (2014). "Standard test method for compressive strength of cylindrical  
420 concrete specimens." ASTM International, West Conshohocken, PA.
- 421 21. ASTM C469 (2014). "Standard test method for static modulus of elasticity and  
422 poisson's ratio of concrete in compression." ASTM International, West  
423 Conshohocken, PA.
- 424 22. ASTM A370 (2012a). "Standard test methods and definitions for mechanical testing  
425 of steel products." ASTM International, West Conshohocken, PA.
- 426 23. ACI (American Concrete Institute). (2013). "Guide to design and construction of  
427 externally bonded fabric-reinforced cementitious matrix (FRCC) systems for repair  
428 and strengthening concrete and masonry structures." ACI 549, Farmington Hills, MI.
- 429 24. ACI (American Concrete Institute). (2014). "Building code requirements for  
430 structural concrete." ACI 318, Farmington Hills, MI.

431 **List of Tables**

432 Table 1- Test matrix for strengthening configuration and anchorage

433 Table 2- Anchor material properties

434 Table 3- Ultimate loads and deflections

435 Table 4- Strain readings in rebars, FRCM sheets, and anchorage

436

437 **List of Figures**

438 **Fig. 1** - FRCM composite materials

439 (a) Polyparaphenylene benzobisoxazole (PBO) mesh

440 (b) Inorganic Matrix

441 (c) Glass fiber

442 (d) Polypropylene fiber

443 **Fig. 2** - Typical geometry and reinforcements of the beam specimen

444 **Fig. 3** - Anchorage systems distribution

445 (a) Glass anchor spikes across the span, bottom view

446 (b) U-wrapped PBO-strips across the span, side view

447 **Fig. 4** - Anchorage systems' details

448 (a) Glass spike

449 (b) Section a-a, U-wrapped PBO strip

450 **Fig. 5** - Glass spikes preparation

451 (a) Folded glass fabric

452 (b) Saturation of glass-fabric end

453 (c) Glass spike

454 (d) Anchor glass spike inside concrete hole

455 **Fig. 6** - FRCM composite application with glass spikes

- 456 (a) Cement-based mortar application
- 457 (b) PBO-sheet embedment into mortar
- 458 (c) Covering PBO-sheet with mortar
- 459 (d) Fan glass spikes
- 460 (e) Covering glass spikes with mortar

461 **Fig. 7** - Anchored U-wrapped PBO strip preparation

- 462 (a) Removal transverse PBO- fabrics
- 463 (b) Geometrical shape of U-wrapped PBO strip
- 464 (c) PBO-fabric ends saturation
- 465 (d) Injection of saturator around PBO strip's end
- 466 (e) U-wrapped PBO strip's end shape

467 **Fig. 8** - FRCM composite application with anchored U-wrapped PBO strips

- 468 (a) Placement of cement-based mortar
- 469 (b) PBO-sheet embedment into mortar
- 470 (c) Application of U-wrapped PBO strip
- 471 (d) Injection of gel epoxy into concrete hole
- 472 (e) Final shape of anchored U-wrapped PBO strip

473 **Fig. 9** - Strain gauges scheme

- 474 (a) Strain gauges distribution for anchored RC beams with glass spike
- 475 (b) Strain gauges distribution for anchored RC beams with U-wrapped PBO

476 **Fig. 10** - Load displacement curves

- 477 (a) Group1, beams with 2-ply

478 (b) Group2, beams with 4-ply

479 **Fig. 11** - Crack pattern and failure mode

ACCEPTED MANUSCRIPT

480

Table 1- Test matrix for strengthening configuration and anchorage

Specimen ID	Layers number	Anchors number	Anchorage configuration	Anchored layer	Anchor type
Con-RC					
G1-2	2				
G1-2-Glass	2	7	Along the span length	2	Glass
G1-2-PBO	2	7	Along the span length	2	PBO
G2-4					
G2-4-Glass	4	7	Along the span length	4	Glass
G2-4-PBO	4	7	Along the span length	4	PBO

481

482 Table 2. Anchor material properties

Reinforcement type	Tensile strength MPa (ksi)	Elastic modulus MPa (ksi)	Ultimate strain mm/mm (in./in.)
PBO fibers, Ruredil Company	5,800 (840)	270,000 (39,160)	0.0215
Glass fibers, D-BASF Company	3,400 (490)	73 (10)	0.045

483

Table 3. Ultimate loads and Displacements

Specimen ID	Experimental ultimate load, kN (kips)	% Increase in load carrying Capacity	Yield displacement ( $\delta_y$ ) mm (in.)	Ultimate displacement ( $\delta_u$ ) mm (in.)	Displacement ductility index ( $\delta_u/\delta_y$ )
Con-RC	122 (27.4)		6.6 (0.26)	51.0 (2.0)	7.7
G1-2	154 (34.6)	26%	4.3 (0.17)	25.4 (1.0)	5.9
G1-2-Glass	146 (33.0)	20%	4.6 (0.18)	30.5 (1.2)	6.7
G1-2-FRCM	148 (33.3)	22%	5.1 (0.2)	25.4 (1.0)	5.0
G2-4	141 (31.6)	15%	5.1 (0.2)	17.8 (0.7)	3.5
G2-4-Glass	154 (34.6)	26%	4.6 (0.18)	28 (1.1)	6.1
G2-4-FRCM	175 (39.2)	43%	4.1 (0.16)	25.4 (1.0)	6.3

484

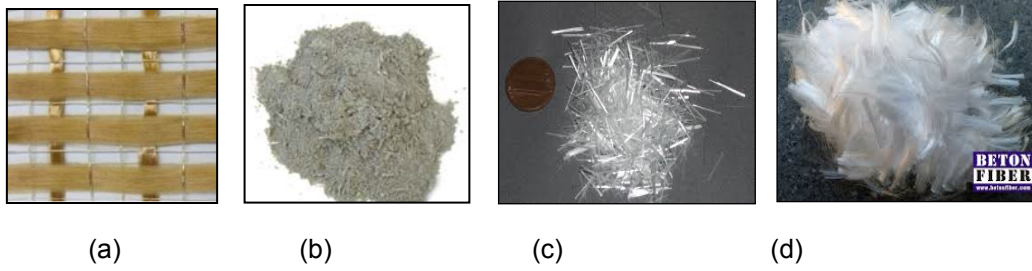


Table 4. Strain readings in rebars, FRCM sheets, and anchorage

Specimen ID	Strain reading, mm/mm (in./in.)					
	Rebar	FRCM sheets at mid-span		FRCM at edge	U-wrapped PBO	
	Mid-span	First sheet	Last sheet	Last sheet	Center	Edge
Con-RC	0.005					
G1-2		0.002	0.005	0.007		
G1-2-Glass		0.005	0.010	0.004		
G1-2-FRCM		0.005	0.004		0.004	0.000
G2-4	0.006		0.006	0.005		
G2-4-Glass		0.004	0.006	0.003		
G2-4-FRCM			0.010		0.010	0.000

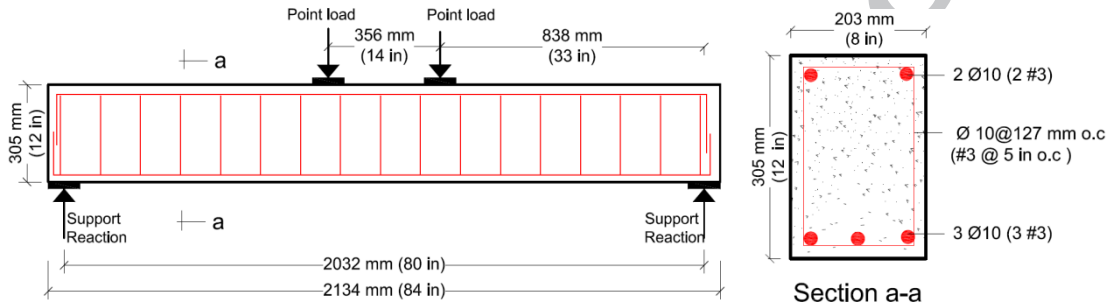
485

ACCEPTED MANUSCRIPT



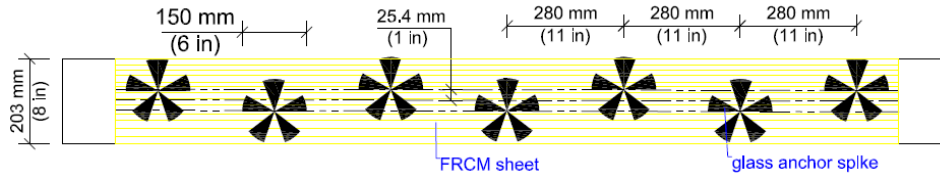
486  
487  
488  
489  
490  
491

Fig. 1 - FRCM composite materials: (a) Polyparaphenylene benzobisoxazole (PBO) mesh, (b) Inorganic Matrix, (c) Glass fiber, and (d) Polypropylene fiber



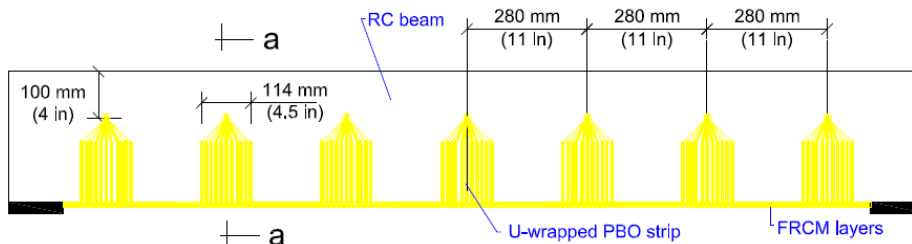
492  
493  
494  
495

Fig. 2 - Typical geometry and reinforcements of the beam specimen



496  
497  
498

(a) Glass anchor spikes across the span, bottom view



499  
500  
501

(b) U-wrapped PBO-strips across the span, side view  
Fig. 3 - Anchorage systems distribution

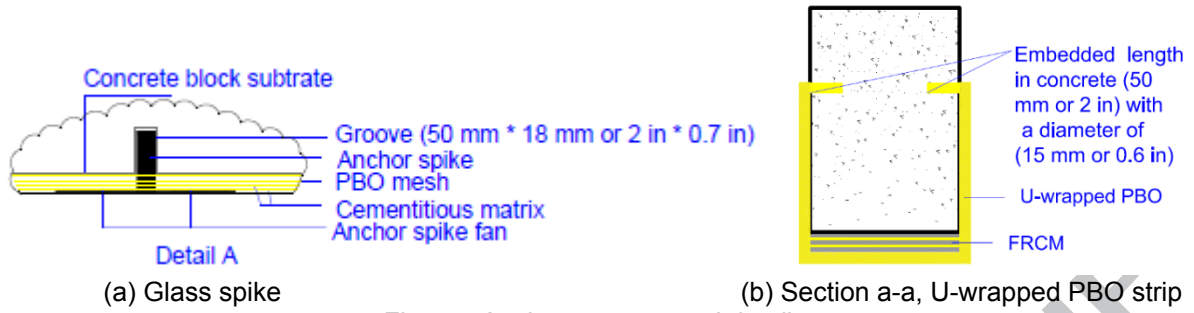


Fig. 4 - Anchorage systems' details

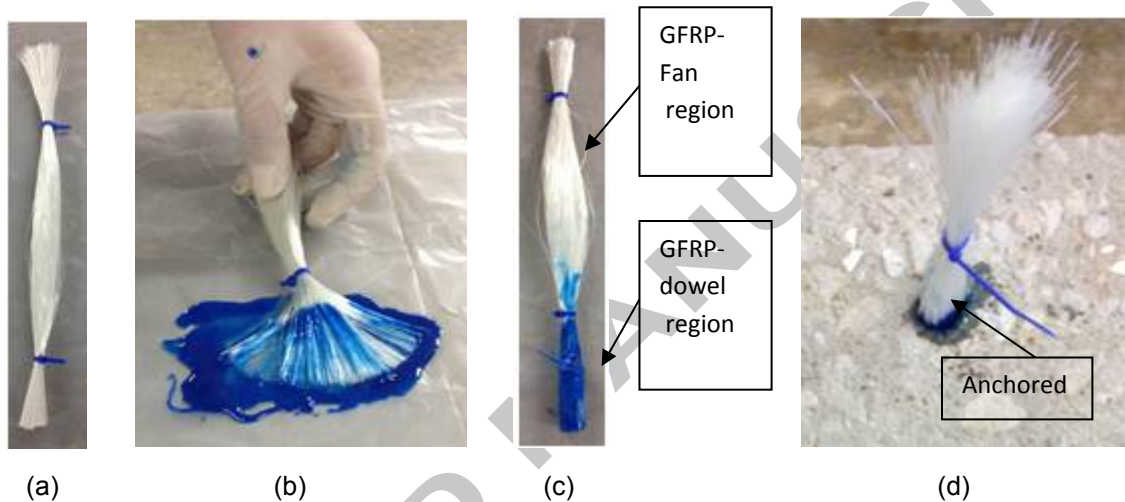


Fig. 5 - Glass spike preparation: (a) Folded glass fabric, (b) Saturation of glass-fabric end, (c) GFRP-dowel region, and (d) Anchored glass spike inside concrete hole

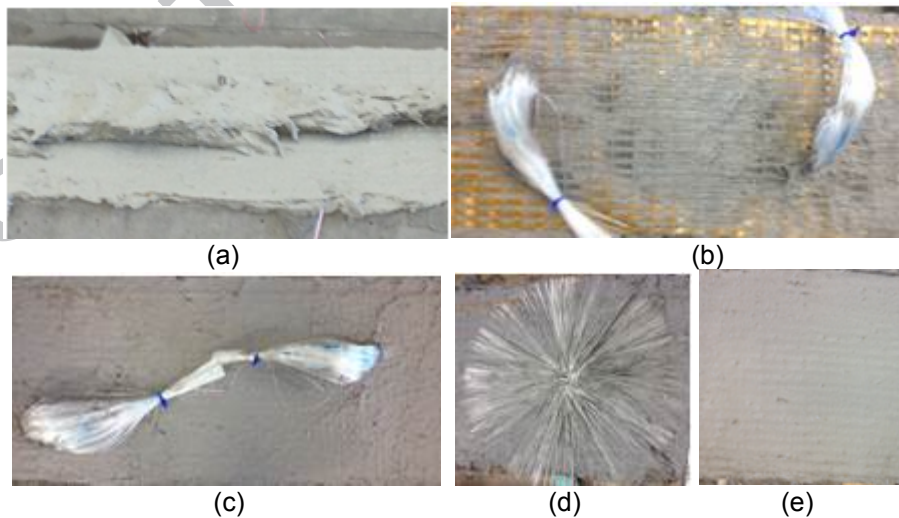
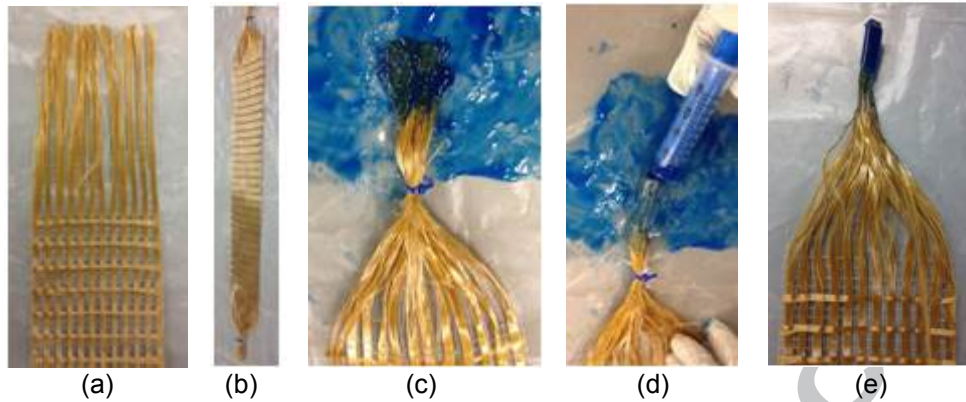


Fig. 6 - FRCM composite application with glass spikes: (a) Cement-based mortar application, (b) PBO-sheet embedding into mortar, (c) Covering PBO-sheet with mortar, (d) Fan glass spikes, and (e) Covering glass spikes with mortar

521



522

523

524

525

526

527

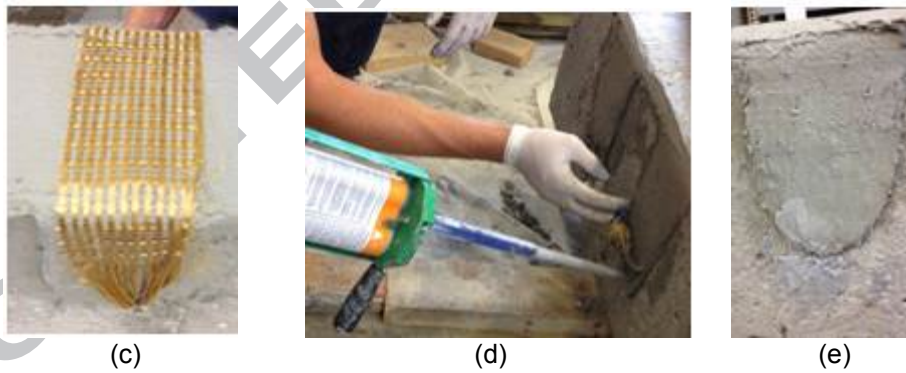
Fig. 7 - Anchored U-wrapped PBO strip preparation: (a) Removal transverse PBO- fabrics, (b) Geometrical shape of U-wrapped PBO strip, (c) PBO-fabric ends saturation, (d) Injection of saturator around PBO strip's end, and (e) U-wrapped PBO strip's end shape

528



529

530



531

532

533

534

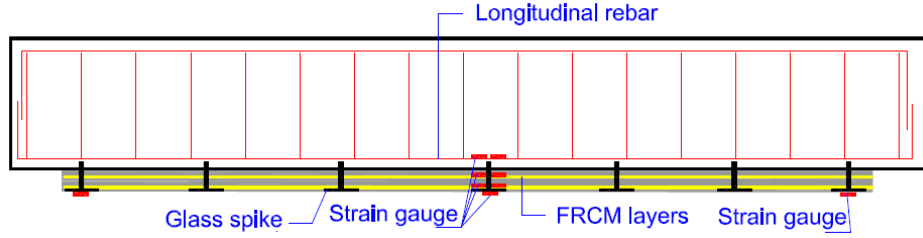
535

536

537

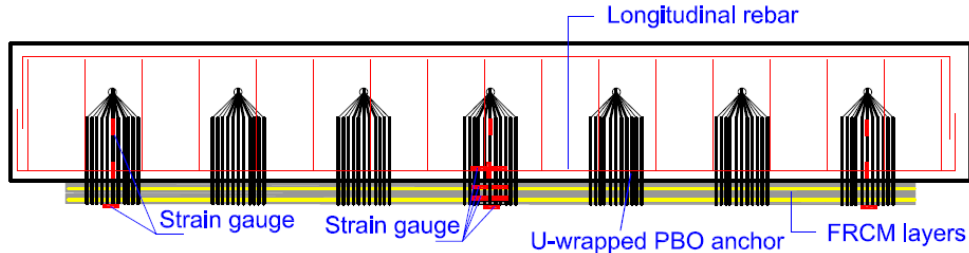
Fig. 8 - FRCM composite application with anchored U-wrapped PBO strips: (a) Placement of cement-based mortar, (b) PBO-sheet embedding into mortar, (c) Application of U-wrapped PBO strip, (d) Injection of gel epoxy into concrete hole, and (e) Final shape of anchored U-wrapped PBO strip

538  
539



(a) Strain gauges distribution for anchored RC beams with glass spike

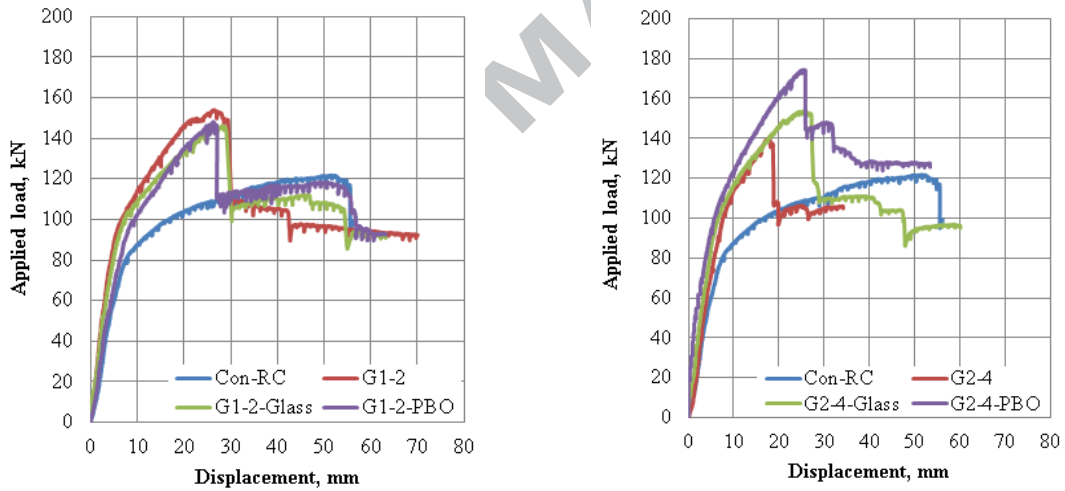
540  
541  
542  
543



(b) Strain gauges distribution for anchored RC beams with U-wrapped PBO

Fig. 9 - Strain gauges scheme

544



(a) Group1, beams with 2-ply

(b) Group2, beams with 4-ply

Conversion units: 1-in. = 25.4 mm; 1 Kip = 4.45 kN

Fig. 10 - Load displacement curves

545  
546  
547  
548  
549  
550



551



552  
553

Con-RC

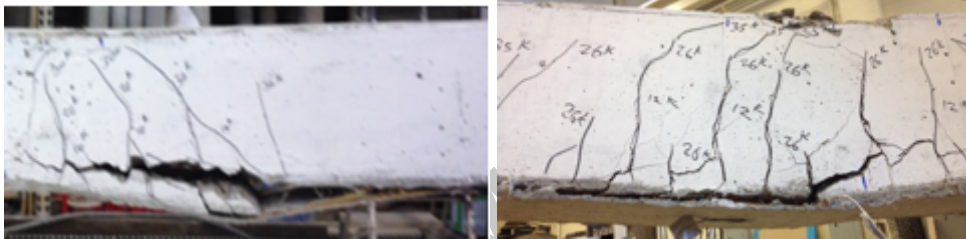
G1-2 (debonding)



554  
555

G1-2-Glass (slippage in PBO)

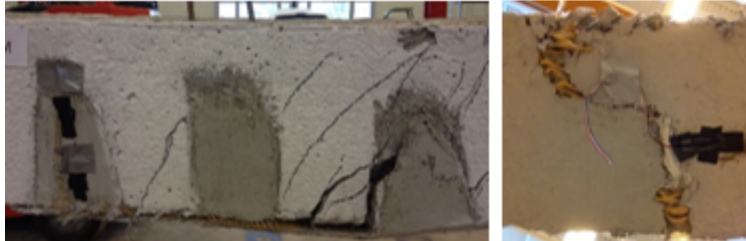
G1-2-FRCM (slippage in PBO)



556  
557

G2-4 (debonding)

G2-4-Glass (debonding)



558  
559  
560  
561

G2-4-FRCM (debonding)

Slippage in PBO

Fig. 11 - Crack pattern and failure mode